Eur. Phys. J. A **4**, 33–39 (1999)

THE EUROPEAN PHYSICAL JOURNAL A

The first excited states of ^{9}Be and ^{9}B

V.D. Efros[1], J.M. Bang[2]

[1] Russian Research Centre "Kurchatov Institute", Kurchatov Square 1, 123182 Moscow, Russia[a]
[2] The Niels Bohr Institute, Blegdamsvej 17, DK–2100 Copenhagen, Denmark[b]

Received: 23 March 1998 / Revised version: 3 September 1998
Communicated by P. Schuck

Abstract. It is found here that the $1/2^+$ first excited state of ^{9}Be is a virtual state with the energy of -23.5 KeV. The line shape for the excitation of the state is approximated with a simple analytic form based on the effective range expansion. The partner in ^{9}B of this state is found to be a resonance with a maximum in the peak at about 1.1 MeV, FWHM of 1.5 MeV, and complex energy of $0.6 - i0.75$ MeV. The line shape for its excitation is calculated in terms of the $p-^8$Be phase shift. The phase shifts are obtained from $N-^8$Be effective potentials deduced from the data on the photodisintegration of ^{9}Be. A possibility for direct extraction of the energy of the resonant state from experimental data is also discussed, and an expression for a residue at a virtual state pole in terms of a quadrature taken over the virtual state eigenfunction is given.

PACS. 21.10.Pc single-particle levels and strength functions – 23.50.+z Decay by proton emission – 24.30.Gd Other resonances – 27.20.+n $6 \leq A \leq 19$ – 03.65.Nk Nonrelativistic scattering theory

1 Introduction

In the present work, we obtain the properties of the first excited states of $A = 9$ nuclei. At low energy these nuclei provide a clean example of three–cluster systems with not easily distortable constituents, thus serving as a test ground for theoretical multicluster approaches, see e.g. [1, 2]. Reliable information on the properties of these nuclei would therefore be very valuable. However, extraction of this information directly from the available experimental data is hampered by their ambiguities. The corresponding data on the low–energy photodisintegration of ^{9}Be are not in mutual agreement, see [3]. All states in ^{9}B are particle unbound which hinders the search for excited states. There exists a long–standing controversy concerning the properties of the ^{9}B first excited state, as obtained both experimentally and theoretically, see [4,5]. Theoretical models can help to analyze the data and also guide future experiments. Along these lines, in [3] a semi–microscopic model to describe the low–energy photodisintegration of ^{9}Be has been developed. An estimation of the reliability of various data sets has been obtained with the help of this model, and a theoretical photodisintegration cross section has been derived for astrophysical applications. The model provides $N-^8$Be effective potentials that reproduce the energy dependence of the cross section. Using them the properties of the first excited state of ^{9}Be are extracted below and estimates for its ^{9}B partner are obtained.

In the next section we elucidate the nature of the first excited state of ^{9}Be and obtain its position. We obtain an analytic form for the line shape of the state and investigate to what degree the line shape is independent of the specific excitation process. In Sect. 3 the first excited state of the ^{9}B nucleus is studied. The expression for the line shape is given, and the position, width and the complex energy of the state are calculated. A possibility to obtain the latter quantity from a direct fit to the line shape is also discussed. In Sect. 4 our results are discussed along with those in the literature.

Our considerations on the shape of the line in Sect. 2 and 3 are of a rather general applicability. In the Appendix a formula expressing a residue at a virtual state pole in terms of a quadrature taken over the virtual state eigenfunction is given.

2 The first excited level of ^{9}Be

We proceed from the dynamic input for the description of the system obtained in [3]. In that work, the ^{9}Be photodisintegration cross section has been calculated in the framework of the following model. The three–body $\alpha + \alpha + n$ representation of the system has been adopted. The ^{9}Be ground state wave function has been calculated from the three–body dynamic equation with $\alpha\alpha$ and αn potentials. The final continuum state has been chosen as a product of

[a] e–mail efros@polyn.kiae.su
[b] e–mail bang@nbivms.nbi.dk

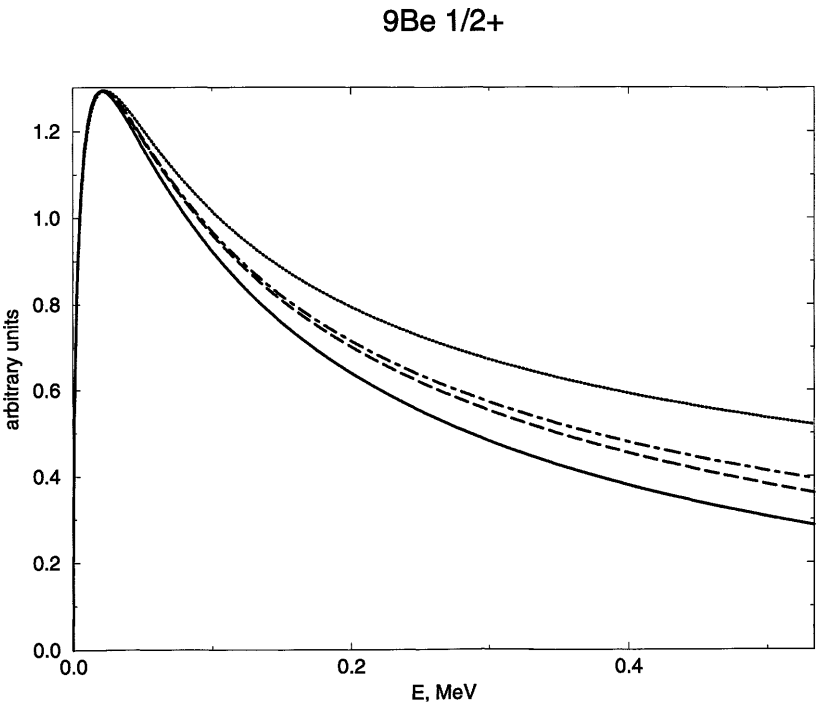

Fig. 1. Line shapes for transitions to the first excited state of ^{9}Be. The solid curve represents the exact line shape for the photodisintegration process calculated with the model of [3]. The long–dashed curve is the energy dependence $k|f(k)|^2$, where f is the $n-^8$Be scattering amplitude. The dash–dotted curve stands for (7). The dotted curve represents the energy dependence given by the second factor from (7)

the intrinsic wave function of the ^{8}Be resonance and the $n-^8$Be relative motion function. The latter wave function has been calculated from the Woods–Saxon potential whose parameters were determined by fitting to several radioactive isotope data.

The model thus gives $n-^8$Be effective potentials that allow extracting the properties of the first excited state of ^{9}Be. First, let us comment on the status of the results obtained in this way. The model accounts for only the two–body $n-^8$Be photodisintegration and disregards the direct three–body $\alpha+\alpha+n$ disintegration. The cross section for the direct $\alpha+\alpha+n$ disintegration is presumably very small due to the threshold regime as also confirmed in experiment, see [3]. Further, the properties of the state considered are determined by the phase shift δ of $n-^8$Be scattering. So, the question arises whether this phase shift can be correctly obtained with the help of the model. In this connection one can admit that in the vicinity of the first excited state of ^{9}Be the energy dependence of the photodisintegration cross section is also determined by this phase shift. To a degree this holds true, use of the two–body ^{8}Be+n dynamics to extract the properties of the state does not contain any restrictions. In [3] the cross section has been fitted for excitation energies up to 0.5 MeV, and in this region the corresponding energy dependence $\sin^2\delta/k$ dominates the cross section, see Fig. 1 below. Moreover, the initial ^{9}Be ground state is described realistically in this model. Therefore, use of the two–body dynamics seems to be sufficient for extracting the properties of the state considered. In general, these properties can also be extracted via the fit of an assumed line shape directly to the data. However, use of the two–body dynamics in conjunction with shell–model considerations allowed selection between alternative data sets in [3]. Below it will also help us to obtain the properties of the analog ^{9}B state relying on the ^{9}Be photodisintegration data.

The fit to the photodisintegration cross section [3] provides the potentials

$$V(r) = V_0/[1+e^{(r-R)/b}] \tag{1}$$

describing $n-^8$Be scattering. The best version

$$V_0 = 35.99 \text{ MeV}, \quad R = 3.126 \text{ fm}, \quad b = 0.8108 \text{ fm} \tag{2}$$

will be used below. Other potential versions lead to similar results as commented below.

Let us denote $E = (\hbar k)^2/(2\mu)$ the energy of the relative $n-^8$Be motion. The potential (1), (2) leads to a $n-^8$Be scattering amplitude $f(k)$ having a pole at $k = -i\kappa$, $\kappa > 0$:

$$f(k) \to \frac{ic_0}{k+i\kappa} \tag{3}$$

as $k \to -i\kappa$. This means that the first excited state of ^{9}Be is a virtual state strongly coupled to the $n-^8$Be channel. The energy of the state is

$$-(\hbar\kappa)^2/(2\mu) = -\bar{E} = -23.53 \text{ KeV}. \tag{4}$$

This value was obtained via solving the eigenvalue problem with the virtual state boundary condition, cf. the Appendix.

Let us consider the shape of the line for a transition proceeding via the virtual state. The shape depends partly on the specific way of excitation of the state. The main energy dependence is universal, however, and it is determined by the intrinsic properties of the state. We shall compare the universal energy dependence to the energy dependence for the process of ^{9}Be photodisintegration and

thus estimate the dependence of the line shape on the specific process.

We assume that the cross section for formation of ^{9}Be in the continuum with the energy E in the vicinity of the excited level can approximately be presented in the form

$$\sigma \sim \int k^2 dk |\langle \Phi | \Psi_k^-(J = 1/2^+)\rangle|^2 \delta(k^2/(2\mu) - E). \quad (5)$$

Here Φ is some localized state in the subspace of the ^{9}Be degrees of freedom. It includes the g.s. of ^{9}Be and the (effective) transition operator accounting for the excitation mechanism (photodisintegration, e.g.). The transition operator may have an energy dependence that is smooth at $E \to 0$. The function Ψ_k^- is the continuum spectrum function that corresponds to incoming n and ^{8}Be fragments in the relative s–state thus describing the two–body ^{8}Be+n photodisintegration. The representation (5) implies that the formation process can be described in the subspace of the ^{9}Be degrees of freedom. Under this condition properties of a state reveal themselves independently of the interactions with other particles participating in its formation.[1] In (5) the normalization condition $\langle \Psi_k^- | \Psi_{k'}^- \rangle = \delta(k - k')/k^2$ should be fulfilled, so that the $n-^8$ Be relative motion function in Ψ_k^- at large distances is normalized to $e^{-i\delta} \sin(kr + \delta)/(kr)$.

We may write the k–integral of (5) as a contour integral where the pole contribution is given by (3), neglecting influence of other degrees of freedom in Φ, Ψ_k^-.

The energy dependence of the cross section (5) in the vicinity of the virtual level is $\sin^2\delta/k$. This energy dependence arises if one replaces the outer part $\sin(kr+\delta)/(kr)$ of the $n-^8$Be relative motion function in the matrix element from (5) by $\sin\delta/(kr)$. This can be done under the conditions $(kR)^2 \ll 1$, and $R \ll |a|$. Here a is the scattering length, and R is chosen such that the relative contribution of $r > R$ values to (5) is small. R exceeds the range of the $n-^8$Be interaction, and the inner part of the final state wave function Ψ_k^- acquires the same energy dependence as the outer one. The $\sin^2\delta/k$ energy dependence is nothing else as the so called Migdal–Watson factor [6].

We can rewrite the corresponding contribution to the cross section as const$\cdot k|f(k)|^2$ where $f(k)$ is the s-wave $n-^8$Be scattering amplitude. Almost the same accuracy is kept if one takes $f(k)$ within the effective range approximation

$$f(k) = [-1/a + (1/2)r_0 k^2 - ik]^{-1}. \quad (6)$$

Then one obtains $|f(k)|^2 \sim [(E + \bar{E})(E + E_1)]^{-1}$. In the model (1), (2) $E_1 = 1.569$ MeV. Using this expression, it is convenient to present the cross section in the following form

$$\sigma(E) = \sigma_m \frac{2\sqrt{E\bar{E}}}{E + \bar{E}} \frac{\bar{E} + E_1}{E + E_1}. \quad (7)$$

Since $\bar{E} \ll E_1$ the energy dependence of the cross section from the threshold up to its maximum is entirely determined by the second factor in (7). It is then seen that the maximum of the cross section occurs practically at the $\bar{E}$ value. With a high precision σ_m is the value of the cross section at the maximum. As one can see from (5) the lowest order correction to (7) is of the form $1 - (E/E_2)$ where E_2 is not small and depends on a specific excitation process. To a certain degree it can be accounted for via a renormalization of E_1. Equation (5) is the Breit-Wigner formula with $\Gamma = \Gamma(E)$, (or, the one-level R matrix expression) rewritten in a different form.

In Fig. 1 various universal expressions for the shape of the line are compared with the exact line shape for the photodisintegration process calculated in the model of [3]. ($E = E_\gamma - E_{th}$.) The full curve represents the latter line shape, the long–dashed curve is the energy dependence $\sim k|f(k)|^2$, the dash-dotted curve represents the expression (7), and the dotted curve is the energy dependence given by the second factor from (7). The FWHM value for the photodisintegration process provided by the first mentioned curve is 196 KeV. The FWHM values provided by the next two curves are 230 and 240 KeV. The latter two values are process–independent. Thus FWHM may have a 20 per cent dependency on the excitation process. On the contrary, the position of the maximum in the peak is practically process–independent coinciding with the absolute value of the energy of the virtual state.

Experimentally, the energy dependence $E^{1/2}(E + \bar{E})^{-1}$, specific to a virtual state could be confirmed by measuring the shape of the line from the threshold up to the region of the maximum with the tagged photon techniques. A simpler, while indirect, way is to study the whole peak in the (e, e') reaction and extract the properties of the state in the way similar to that used above for photodisintegration. In case of accurate and detailed (e, e') or (p, p') data the energy $\bar{E}$ of the state could also be extracted from the fit of the (7) form or its above–mentioned extension.

Besides the energy $\bar{E}$, or the pole position of the $n-^8$Be scattering amplitude, another quantity to be reproduced in a microscopic calculation is the residue c_0 in the pole, (3). The exact c_0 value was calculated with the formula derived in the Appendix that represents c_0 as an integral taken over the virtual state eigenfunction. The result is $c_0 = 0.7837$. We note that with high accuracy both $\bar{E}$ (or κ, see (4),) and c_0 can be expressed in terms of the $n-^8$Be scattering length a and the effective range r_0 . From (6) one obtains

$$\kappa = r_0^{-1}[(1 - 2r_0/a)^{1/2} - 1],$$
$$c_0 = (1 - 2r_0/a)^{-1/2} = (1 + \kappa r_0)^{-1}. \quad (8)$$

The effective range parameters for the potential (1), (2) are

$$a = -27.65 \text{ fm}, \qquad r_0 = 8.788 \text{ fm}, \quad (9)$$

[1] In the framework of the model [3] only the two–body ^{8}Be+n channel is retained in the function Ψ_k^- while the incoming three–body $\alpha + \alpha + n$ channels are disregarded. This model assumption is also inherent to all the previous work. One can see, however, that to a first approximation this does not change the energy dependence of the cross section and thus does not influence the results

and the expected accuracy of the above expressions is about $|r_0/a|^3 \simeq 1\%$. Their numerical values proved to be even more accurate: $\bar{E} = 23.51$ KeV, $c_0 = 0.7819$. As it is explained in [3] all other acceptable potentials found there lead to the a and r_0 values very close to those in (9). Hence the properties of the virtual state given by these potentials are quite similar.

3 The first excited level of ^{9}B

To calculate the resonant peak for an excitation of the ^{9}B $1/2^+$ level, we proceed again from (5), only with a different expression for the pole term but still assuming that there is only one decay channel, $p-^8$Be, for the state considered. In the ^{9}B case, disregarding the possibility for the decay into the $N+\alpha+\alpha$ channel, being less substantiated than in the ^{9}Be case because of a higher energy with respect to the three–body threshold, seems still to be reasonable. The $n-^8$Be potentials obtained in [3] lead presumably to a good description of the $n-^8$Be $1/2^+$ phase shifts. Then one may suggest that the $p-^8$Be $1/2^+$ phase shifts will also be properly reproduced with these potentials with an addition of the Coulomb interaction. This will suffice to obtain approximately the main properties of the ^{9}B $1/2^+$ level.

Beyond the range of the nuclear potential the $p-^8$Be relative motion function $\chi(r)/kr$ entering Ψ_k^- in (5) may be represented in the form

$$\chi = G\sin\delta + F\cos\delta = (\sin\delta/C)[C(G + F\cot\delta)] \equiv (\sin\delta/C)\phi(k,r). \quad (10)$$

Here δ is the nuclear phase shift, $C^2 = 2\pi\eta[\exp(2\pi\eta) - 1]^{-1}$ is the Coulomb penetrability factor, and F and G are the Coulomb functions. The possible resonant pole is contained in the factor $\sin\delta$ while the function ϕ defined in (10) is smooth at low energies. (At $k \to 0$ $\phi(k,r) \to zK_1(z) - (a_c/4a)zI_1(z)$, $z = 2(2r/a_c)^{1/2}$, where a is the scattering length, and a_c is the Bohr radius.) To a first approximation one may use $\phi(k_0,r)$ in the calculation of the cross section (5), k_0 being chosen in the vicinity of the resonance. Hence the energy dependence of the excitation cross section in the resonant peak region is given by the expression

$$\frac{\sin^2\delta}{kC^2} = k\frac{|f(k)|^2}{C^2} = \frac{kC^2}{(kC^2\cot\delta)^2 + (kC^2)^2}. \quad (11)$$

Here f is the nuclear amplitude of $p-^8$Be scattering. Thus, quite naturally, up to process–dependent corrections the resonant cross section for the excitation of the state is proportional to the scattering cross section times a universal factor proportional to a width. The quantity $kC^2\cot\delta$ in (11) allows the well–known representation $[-1/a + (1/2)r_0k^2 + \ldots] - (2/a_c)h(1/a_ck)$, showing that it is smooth and finite at $E = 0$. The kC^2 behavior of the cross section at $E \to 0$ is seen directly from (5) and the properties of the Coulomb functions.

The $p-^8$Be phase shifts entering (11) were obtained from the Schrödinger equation with the nuclear potential (1), (2) plus the Coulomb interaction. The latter took into account the density distribution in ^{8}Be and the charge distribution in the α particles:

$$V_{Coul}(r) = (4e^2/r)(2/\pi)\int_0^\infty (\sin qr/q)F_\alpha(q)I(q)dq, \quad (12)$$

where $F_\alpha(q)$ is the charge form factor of the α particle [7], and

$$I(q) = \int_0^\infty (2/q\rho)\sin(q\rho/2)\psi^2(\rho)d\rho,$$

ψ being the ^{8}Be wave function.

The energy dependence (11) obtained indeed proved to exhibit a pronounced peak, and it is shown in Fig. 2 with a solid curve. The position E_{max} of the maximum in the peak with respect to the $p-^8$Be threshold and the FWHM value are the following: E_{max} =1.13 MeV, FWHM=1.64 MeV. The long–dashed curve in Fig. 2 represents the peak for the other acceptable nuclear potential of the Woods–Saxon form found in [3] whose parameters are

$$V_0 = 52.86 \text{ MeV}, \quad R = 2.006 \text{ fm}, \quad b = 1.051 \text{ fm}. \quad (13)$$

For this case $E_{max} = 1.02$ MeV, and FWHM=1.43 MeV.

If the peak obtained corresponds to a state then the scattering amplitude should have a pole in the vicinity of E_{max}. Thus we shall search for such a pole. One can show that when the long–range Coulomb interaction is switched on, virtual states cease to exist, turning normally to complex–energy resonances, and this applies to our case. (It applies also to, e.g., $p--p$ scattering where, in contrast to what is often said, there are no virtual states.) The energy $E = E_0 - i\Gamma/2$ of a resonance being connected to the pole of a scattering amplitude, is process–independent and thus characterizes a resonance quite precisely even in case of a broad width.

In our case this quantity is computed as a complex eigenvalue in the $p-^8$Be Schrödinger equation. Here we used the codes of [8] or, when this is inoperative, the ρ–series (14.1.4) for F and the corresponding expansion (14.1.14) – (14.1.19) for G from [9].[2] These expansions are fast convergent for not extremely high values of $|\rho|$, $|\eta|$.

The resonant pole was found with the following parameters: $E_0 = 0.60$ MeV, $\Gamma/2 = 0.77$ MeV, and $E_0 = 0.56$ MeV, $\Gamma/2 = 0.70$ MeV for the potentials (2) and (13), respectively. The positions E_0 of the resonance are shifted downwards with respect to the maxima in the peak found

[2] We rewrite the latter expansion for $l = 0$ in the form valid for complex η values:

$$G(\eta,\rho) = C^{-1}\{2\eta\rho\Phi(\eta,\rho)[\ln(2\rho) + (1/2)[\psi(i\eta) + \psi(-i\eta)] + 2\gamma - 1] + \sum_{k=0}^{\infty} a_k(\eta)\rho^k\}.$$

Here $\psi(z) = \Gamma'(z)/\Gamma(z)$, γ is the Euler constant, and the quantities $\Phi(\eta,\rho)$ and $a_k(\eta)$ are defined in [9]

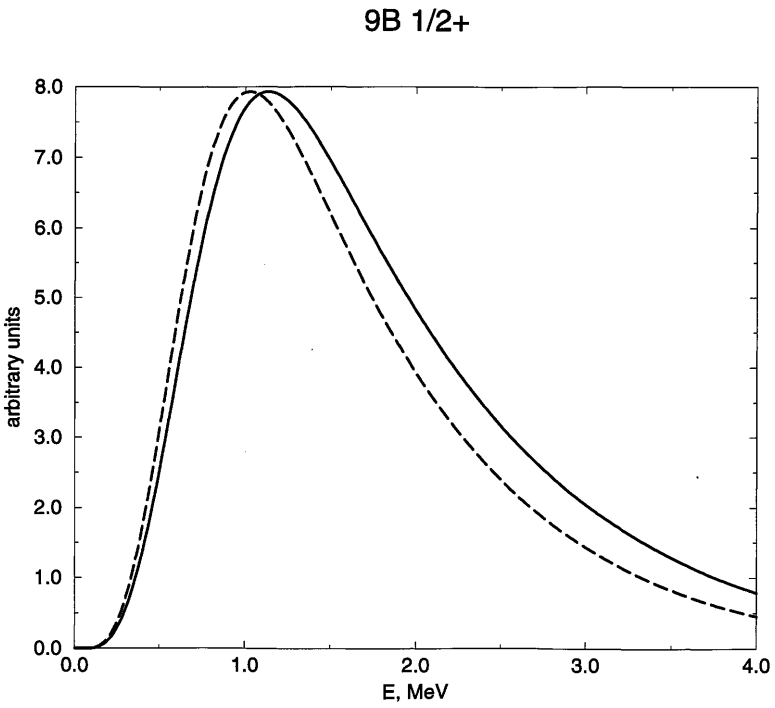

Fig. 2. Line shapes for transitions to the first excited state of ^{9}B calculated according to (11). The solid and long–dashed curves are for the potentials with the parameters (2) and (13), respectively

above, while the widths Γ are close to the FWHM values. Similar trends were observed for ^{5}He, ^{5}Li resonances [10]. It is interesting to note that the height of the Coulomb barrier in our case proved to be 0.63 MeV only, i.e. the resonance with a finite width sits at the top of the barrier. This is possible only when the width of the resonance becomes so broad that it is comparable to E_0.

In conclusion, let us add the following two comments. First, since the energy $E = E_0 - i\Gamma/2$ of the resonance is a convenient process–independent quantity to compare with theory, it would be very useful to extract it directly from future experimental data without constructing a model for the excitation process. Such a task has been accomplished successfully in some cases, see e.g. [10,11]. However it is not clear whether this is possible in practice for the broad resonance we consider. We perform a numerical experiment to clarify this issue. We explore the possibility to reconstruct the E_0 and Γ values obtained proceeding from a reasonable fit to the resonant peak of the form (11), see Fig. 2, calculated in the same model, (2). We fit the peak with the expression

$$a_1 \frac{kC^2}{[a_2 + a_3(E - E') + a_4(E - E')^2]^2 + (kC^2)^2} \qquad (14)$$

related to (11). Here $E' = 1.5$ MeV, the fit is extended over the values $(E' - \Gamma/2) \le E \le (E' + \Gamma/2)$ at which the cross section exceeds a half of its value at the maximum, and a_i are fitting parameters. Choosing the form of the expression (14) it was taken into account that the effective range approximation is not accurate enough in the peak region and that $kC^2 \cot\delta$ has no minimum in that region in our case. The resonant E value, $E = E_0 - i\Gamma/2$, is obtained as a zero of the expression $a_2 + a_3(E - E') + a_4(E - E')^2 - ikC^2$ that corresponds to the pole of the scattering amplitude.

The search of the least square minimum was performed with respect to E_0, Γ, and a_3 with values taken on some grids. At given values of these parameters a_2 and a_4 were fixed via equating to zero real and imaginary parts of the above expression. The a_1 value was found analytically from the least square minimum requirement. (If $kC^2 \cot\delta$ is completely reproduced by the fit, we should have $a_1 = 1$.)

It occurred that the fit is unstable in this form, and a_1 takes unrealistic values. Let us then remove the search of the Γ value admitting instead the hypothesis Γ =FWHM. This condition is fulfilled with sufficient accuracy in our case, and also in the ^{5}He, ^{5}Li cases [10]. This modified procedure leads to E_0 values that are quite stable and close to the true one. The stability was checked by changing the stepsize in the a_3 parameter.

The second comment concerns the value of the effective range r_0 for the $p-^8$Be scattering. For the potential (2), for example, it proved to be 3.01 fm i.e. much smaller then that from (9) for the $n-^8$Be case. This, however, does not mean that the range of the $p-^8$Be nuclear interaction is sizably different from that for the $n-^8$Be interaction. The effective range can serve as a measure of the interaction range when $a \gg r_0$ and, in addition, the zero energy scattering wave function $u(r)$ entering the effective range definition is close to unity at the edge of the well R. This holds true for the neutral case but not when the rather strong Coulomb interaction is present. The latter interaction suppresses the wave function at the R value, so that the range of nuclear interaction may be estimated as $r_0/u^2(R)$.

4 Discussion

Basing on the model of [3] we obtained that the first excited level of ^{9}Be is a virtual state with the energy $-\bar{E}$ =- 23.5 KeV with respect to the $n-^9$Be threshold. It is shown that the peak position for an excitation of this state practically coincides with the $\bar{E}$ value while the FWHM value of the peak may sizably depend on a specific excitation process. Within the effective range approximation the properties of the state are reproduced with a high accuracy. The line shape is aproximated with a simple analytic form based on the effective range expansion.

In [12] a single–level R-matrix fit to the photodisintegration data of [13] led to the description of the state considered as a complex–energy resonant state. However the data [13] are at variance with the earlier data, and it was concluded in [3] that the latter ones are preferable. The positions of maxima in the available experimental ^{9}Be(p,p') spectra [14,15] do not contradict the above listed value of 23.5 KeV.

In [15] the quantities pertaining to the $1/2^+$ state of ^{9}Be were presented in the form of parameters entering the Breit–Wigner formula

$$\sigma(E) = \frac{8\pi^2}{9}\frac{e^2}{\hbar c}E_\gamma B(E1,E_\gamma) \times \frac{\Gamma(E)/2}{(E-E_R)^2+[\Gamma(E)/2]^2}, \qquad (15)$$

that was fitted to the (e,e') data of that paper. Here $\Gamma(E) = G\sqrt{E}$, G being the reduced width of the level. The values $E_R = 19 \pm 7$ KeV, $\Gamma = 217 \pm 10$ KeV were reported, the latter value refers presumably to $\Gamma(E_R)$. These values are quoted in the review article [16]. They cannot be correct since they lead to a quite unrealistic $\bar{E}$ value, i.e. that of the maximum of an excitation cross section, of 0.6 KeV. Based on Fig. 6 from [15] one may suggest, however, that these values do not refer to E_R and Γ from (15) but to the position of the maximum of the cross section and the FWHM, respectively. If it is the case, these values are in agreement with ours. (Absence of the information on energy dependence of $B(E1,E_\gamma)$ inhibits a precise conclusion concerning the FWHM.)

In [1] a microscopic study of the spectrum of ^{9}Be at the 9–nucleon level was undertaken. The $1/2^+$ level was not detected at all. The reason may lie in that the method of complex scaling used in that work is suited for search of complex–energy resonant states but not virtual states.

Further, we studied the first excited state in ^{9}B in the present work using the nuclear potentials derived in [3] from the analysis of the ^{9}Be photodisintegration data and adding the Coulomb interaction between p and ^{8}Be. An approximate process–independent expression for the line shape of the state in terms of the $p-^8$Be phase shift is obtained. The position of the peak with respect to the $p-^8$Be threshold and its FWHM given by this expression are about 1.1 MeV and 1.5 MeV, respectively. The peak considered is caused by a complex–energy pole in the $p-^8$Be scattering amplitude. The pole proved to be located at energy $E = E_0 - i\Gamma/2$ with $E_0 \simeq 0.6$ MeV and $\Gamma \simeq 1.5$ MeV.

In [4] a prediction for the peak of the ^{9}B resonance was obtained: E_{max} = 1.13 MeV, FWHM=1.40 MeV. It is close to ours while the underlying assumptions of that work were rather different. Our common features with that work consist in use of $p-^8$Be dynamics to obtain the resonance and in obtaining the $p-^8$Be Woods–Saxon potential from ^{9}Be photodisintegration data. The big differences consist in the conditions from which parameters of the potential are deduced, in the parameters themselves, and in a prescription to calculate the resonance. In [4] the two–body dynamics were used both for the inital ground state and the final continuum state of ^{9}Be. Depths of the potentials were varied whereas their range and diffuseness were kept at their "classic" vaues. The data of [13] were fitted (probably up to a normalization). The fit was only moderately good. The line shape of the ^{9}B resonance was computed as if it were excited due to a fictitious dipole transition from the ground state of ^{9}Be. Our potentials were deduced [3] at the assumption of three-body $\alpha+\alpha+n$ dynamics for the ground state of ^{9}Be and two–body dynamics for its continuum. Range and diffuseness of the potential were varied in addition to the depth. The data of [13] were concluded to be less preferable, and the alternative earlier data were fitted without freedom in an absolute normalization. The fit is statistically quite good. The line shape of the ^{9}B resonance was computed from (11). The Coulomb interaction was treated more accurately, and also the pole position $E_0 - i\Gamma/2$ was calculated. Keeping range and diffuseness of the potential at their "classic" values was perhaps an important point in the analysis of [4] which allowed obtaining correct results even at assumptions that are not completely valid. An interesting point is that the different prescriptions for calculating a resonance in our work and in [4] lead to similar results. To check this we calculated the resonance for the potential of [4] with the prescription of (11). The results are E_{max} = 1.06 MeV, FWHM=1.47 MeV, and they are close to those reported in [4]. (The difference in treatment of the Coulomb interaction should also be taken into account here.)

In [17] the energy of the $1/2^+$ first excited state of ^{9}B was derived from R–matrix parameters fitted [12] to the ^{9}Be data of [13] and from values of the Coulomb displacement energy calculated with the help of the shell model. The result $E_0 \simeq 2$ MeV differs considerably from that of our work and [4] leading to the inverted value of the so called Thomas–Ehrmann shift. As it is mentioned above in connection with our comparisons to Refs. [12,4], use of this particular set of data to derive R–matrix parameters might be a disadvantage.

We are indebted to M.V. Zhukov for useful discussion in the course of this study. A part of this work was done during the stay of V.D.E. at the Niels Bohr Institute, and he expresses his gratitude for the kind hospitality. The work was partially supported by Russian Foundation for Basic Research (grants 96-15-96548 and 97-02-17003).

Appendix
Residue properties of virtual state poles of a scattering amplitude

In the vicinity of the virtual state pole the two–body scattering amplitude behaves according to (3). We obtain a formula that expresses a residue c_0 in terms of a quadrature taken over the virtual state eigenfunction. The result is $c_0 = (-1)^l/I_v$, where I_v is given by (A4) below with $\Delta(r)$ entering the virtual state eigenfunction (A3). The latter function is readily calculated from the Schrödinger equation. (The consideration is formally applicable to a motion in a central potential with any orbital momentum l although the $l > 0$ virtual state case is of little interest.)

Let $\psi(r)$ be the solution to the Schrödinger equation regular at the origin. Beyond the range of a potential the function $\chi(r) = r\psi(r)$ behaves as $\exp(ikr) + (-1)^{l+1}S^{-1}(k)\exp(-ikr)$. Complex k values are allowed. A virtual state corresponds to a pole of the S–matrix $S(k)$ at $k = -i\kappa$, κ being real and positive.[3] In terms of κ, $\chi(r) = \exp(\kappa r) + (-1)^{l+1}S^{-1}\exp(-\kappa r)$ at large r, so the boundary condition for virtual states consists in absence of the decreasing exponential. If the eigenvalue is sufficiently small then the eigensolution can be found directly using a logarithmic derivative at sufficiently large r. This holds true in our case.

For bound states, the well–known formula corresponding to that we want to derive is the following [18,19]. Let the bound state wave function be normalized to unity, and A the coefficient in its asymptotics $A\exp(-\kappa r)$. Then

$$f(k) \to \frac{i(-1)^l A^2}{2\kappa}\frac{1}{k - i\kappa} \qquad \text{(A1)}$$

as k tends to $i\kappa$.

In the virtual state case we shall proceed from the relation

$$\frac{\partial\chi}{\partial r}\frac{\partial\chi}{\partial E} - \chi\frac{\partial^2\chi}{\partial r\partial E} = \frac{2m}{\hbar^2}\int_0^r \chi^2(r')dr'. \qquad \text{(A2)}$$

It is similar to that used in [6] for the derivation of (A1). We take r to be large enough so that in the vicinity of the virtual state pole $\chi(r, E) \simeq \exp(\kappa r) + \alpha(E + \bar{E})\exp(-\kappa r)$. Here $\bar{E} = (\hbar\kappa)^2/2m$. The pole term in the scattering amplitude is then $(-1)^{l+1}(2\kappa\alpha)^{-1}(E + \bar{E})^{-1}$, and the constant α is to be found. We denote $\chi_v(r)$ the virtual state eigenfunction, so that $\chi_v = \chi(E = -\bar{E})$. We set

$$\chi_v(r') = \exp(\kappa r') + \Delta(r'). \qquad \text{(A3)}$$

Here $\Delta(r)$ is a rapidly decreasing function. We substitute (A3) into the right–hand side of (A2) and equate the terms of the orders of $\exp(\kappa r)$ and unity in both sides of (A2) at E tending to $-\bar{E}$. Then we obtain $2\kappa\alpha = -(2m/\hbar^2)(I_v/2\kappa)$, with

$$I_v = 1 - 2\kappa\int_0^\infty [\Delta^2(r) + 2\Delta(r)\exp(\kappa r)]dr. \qquad \text{(A4)}$$

The product $\Delta(r)\exp(\kappa r)$ is a rapidly decreasing function, so the integral converges. Finally,

$$f(k) \to \frac{i(-1)^l}{I_v}\frac{1}{k + i\kappa} \qquad \text{(A5)}$$

as k tends to $-i\kappa$, $\kappa > 0$.

To display an analogy between the bound and virtual state pole cases, we note that the right–hand side of (A1) can be rewritten as

$$\frac{i(-1)^l}{2\kappa N_b}\frac{1}{k - i\kappa}, \qquad \text{(A6)}$$

where N_b is the norm of the eigenfunction χ_b behaving as $\exp(-\kappa r)$ at r tending to infinity. If one sets $\chi_b(r) = \exp(-\kappa r) + \Delta(r)$ then $2\kappa N_b$ takes just the form of (A4) with the replacement $\kappa \to -\kappa$.

[3] It is implied that at large r the potential decreases more rapidly than $\exp(-\kappa r)$, cf [6]

References

1. K. Arai, Y. Ogawa, Y. Suzuki, and K. Varga, Phys. Rev. C **54**, 132 (1996)
2. V.T. Voronchev, V.I. Kukulin, V.N. Pomerantsev, and G.G. Ryzhikh, Few–Body Sys. **18**, 191 (1995)
3. V.D. Efros, H. Oberhummer, A.V. Pushkin, and I.J. Thompson, Eur. Phys. J. A **1**, 447 (1998)
4. R. Sherr and G. Bertsch, Phys. Rev. C **32**, 1809 (1985)
5. M.A. Tiede, et al., Phys. Rev. C **52**, 1315 (1995); F.C. Barker, Phys. Rev. C **53**, 2539 (1996)
6. L.D. Landau and E.M. Lifshitz, *Quantum Mechanics* (Oxford, Pergamon Press 1977)
7. C.R. Ottermann, et al., Nucl. Phys. **A436**, 688 (1985)
8. I.J. Thompson and A.R. Barnett, Comp. Phys. Com. **36**, 363 (1985)
9. M. Abramovitz and I.A. Stegun, *Handbook of Mathematical Functions* (Dover, N.Y. 1970)
10. V.D. Efros and H. Oberhummer, Phys. Rev. C **54**, 1485 (1996)
11. G.M. Hale, R.E. Brown, and N. Jarmie, Phys. Rev. Lett. **59**, 763 (1987)
12. F.C. Barker, Can. J. Phys. **61**, 1371 (1983)
13. M. Fushiro, et al. Can. J. Phys. **60**, 1672 (1982)
14. S.N. Tucker, P.B. Treacy, and V.V. Komarov, Aust. J. Phys. **23**, 651 (1970)
15. G. Kuechler, A. Richter, and W. von Witsch, Z. Phys. A**326**, 447 (1987)
16. F. Ajzenberg–Selove, Nucl. Phys. **A490**, 1 (1988)
17. F.C. Barker, Aust. J. Phys. **40**, 307 (1987)
18. H.A. Kramers, Hand und Jahrbuch der Chemisher Physik **1**, 312 (1938)
19. W. Heisenberg, Z. Naturforsh. **1**, 608 (1946); C. Möller; Dan. Vid. Selsk. Mat. Phys. Medd. **22**, N19 (1946); N. Hu, Phys. Rev. **74**, 131 (1948)